# ARTICLE IN PRESS

# Harmony search algorithm for image reconstruction from projections

Q1 Ahlem Ouaddah*, Dalila Boughaci

University of Science and Technology Houari Boumediene (USTHB), Electrical Engineering and Computer Science Faculty, Department of Computer Science,
LRIA Laboratory, El-Alia BP 32 Bab-Ezzouar, 16111 Algiers, Algeria

## ABSTRACT

Image reconstruction from projections is an important problem in the areas of microscopy, geophysics, astrophysics, satellite and medical imaging. The problem of image reconstruction from projections is considered as an optimization problem where a meta-heuristic technique can be used to solve it. In this paper, we propose a new method based on harmony search (HS) meta-heuristic for image reconstruction from projections. The HS method is combined then with a local search method (LS) to improve the quality of reconstructed images in tomography. The two proposed methods (HS and hybrid HS) are validated on some images and compared with both the filtered back-projection (FBP) and the simultaneous iterative reconstruction technique (SIRT) methods. The numerical results are encouraging and demonstrate the benefits of the proposed methods for image reconstruction in tomography.

© 2016 Elsevier B.V. All rights reserved.

## 1. Introduction

Image reconstruction from projections is an important problem that has been handled by a large number of scientists. This technical has found widespread application in many scientific fields, including microscopy, geophysics, astrophysics and medical imaging [1–3].

Let us consider a set of measures produced by unknown object, image reconstruction from projections is an inverse problem that consists in finding the original object from its projections. The problem is also ill-posed because the solution could be unique, could not exist, or different solutions could exist for the same problem [4].

The X-ray computed tomography (CT) is the most familiar application of image reconstruction from projections. The X scanners are used in different areas such as medical routine, metallurgy, material structure analysis and others [5]. The principle of CT has expanded to other physical phenomena that X-rays as radioactive emission (tomographic emission to a single photon (SPECT) or positron emission tomography (PET)), ultrasound, microwave, electrical impedance and magnetic resonance imaging (MRI).

The problem of image reconstruction from projections is an important problem in tomography. Several methods for image reconstruction are proposed in CT. Among them, we mention the following ones: filtered back-projection method (FBP) [6], algebraic reconstruction techniques (ART) [7], maximum likelihood expectation maximization (MLEM) [8] and simultaneous iterative reconstruction technique (SIRT) [9]. However, till now there is no method able to give satisfactory results. Other iterative methods were recently proposed as model-based iterative reconstruction (MBIR) [10] or iterative reconstruction in image space (IRIS) [11].

Some researchers [12,13,1,14–18] consider this problem as an optimization problem where the aim is to minimize a certain objective function referred to the projections.

The meta-heuristic is a kind of methods that have been used with success in solving several optimization problems in many search areas such as geophysics, astrophysics, medical imaging and microscopy [19–22]. However, to the best of our knowledge, there are only a few researches on tomographic reconstruction by using meta-heuristics based approaches. We can cite, for example the genetic and fly algorithms for tomographic reconstruction [23,17,13,14,16]. These methods are till now in the experimental stage. Nonetheless, it is possible to further improve the reconstruction.

The aim of the current work is to open a new field by using harmony search based meta-heuristic in image reconstruction. Further, we hope to improve the quality of reconstruction and find a method able to solve efficiently the considered problem of image reconstruction. First, we propose a new method based on harmony search (HS) meta-heuristic for image reconstruction in tomography. Then, we combine HS with a local search method (LS) to enhance the performance for image reconstruction with low

* Corresponding author. Tel.: +213 550324175.
E-mail addresses: aouaddah@usthb.dz (A. Ouaddah), dboughaci@usthb.dz (D. Boughaci).
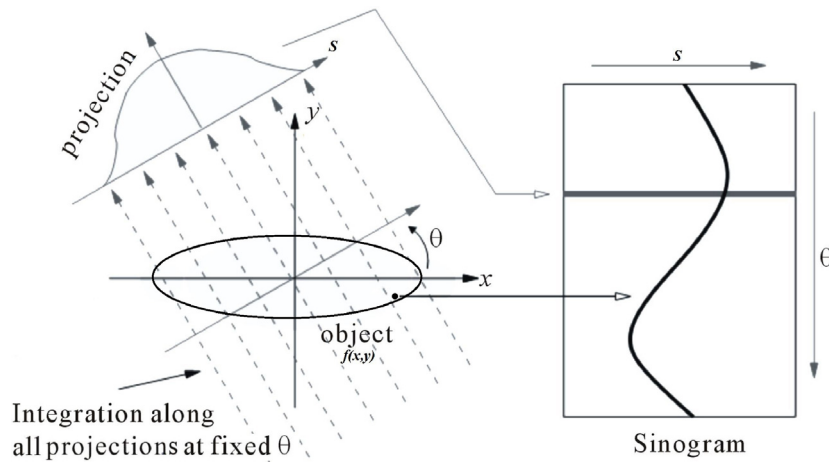
**Fig. 1.** Example of process of measuring projections and recording as sinogram [28].

resolution [18]. The two proposed methods are compared with FBP analytical method which is till now largely implemented in CT clinical routine [24,25] and with the iterative technique SIRT.

The rest of the paper is organized as follows: Section 2 presents a background on some basic principles of reconstruction from projections with an overview of standard methods for reconstruction in tomography. Section 3 details the proposed approaches for image reconstruction from projections. Section 4 gives experiments and some numerical results. Finally, we conclude in Section 5 and give some future works.

## 2. Background

Tomography is an imaging technique that permits to visualize the internal structure of an object. Tomography is performed in two steps. The first step is the process of data acquisition for recording projections. The set of angular projections is called *sinogram*. This *sinogram* is used in the second step to reconstruct the image. There are two main groups of reconstruction methods: the analytic and the iterative reconstruction methods.

*The aim of this section is to give a background on basic principles of tomographic reconstruction followed by a brief description of standards methods applied in this field.*

### 2.1. Basic principles of reconstruction from projections

The first step in tomography is the data acquisition process that can be modeled by Radon transform [5]. This transform converts a 2D function $f(x,y)$ to 1D projection following a Cartesian coordinates $(s,\theta)$ [15]. In continuous cases, projections $P(s,\theta)$ with $s$ the distance between each point crossed by the projection ray and the center of $\theta$ angle, such as (1), is to measure the integral of an infinite domain of all points $(x, y)$ of the function or the object $f(x, y)$ [26,27]. These points contribute in $P$ projection such as (2).

$$s = x\cos(\theta) + y\sin(\theta) \tag{1}$$

$$P(s, \theta) = \int_{-\infty}^{+\infty} f(x, y)dv \tag{2}$$

The set of these projections acquired at different angles $\theta$ are recorded into a certain format so-called *sinogram*. A *sinogram* is simply the 2D array of data containing the projections. Each column of the sinogram corresponds to the set of acquired projections for the same radial value $s$ at different angles.

The two images depicted in Fig. 1 explain the process of data acquisition. The left image corresponds to the acquisition of the

projections from the objects and the right one corresponds to projections collected as sinogram.

By analogy, in the discrete case, Radon transform is the sum of the values of all pixels $(x, y)$ that contribute in each projection $P_i$ as given in formula (3); $r_{ij}$ is the value of pixel contribution $j$ at the projection $P_i$; $f_j$ is the value of this pixel [29].

$$P_i = \sum_{j=1}^{m} r_{ij}f_j \tag{3}$$

Added to this transform, John Radon has proved in 1917, that the reconstruction of the object from its projections is possible and could be exact if we have an infinite number of projections, and in reality it is impossible [30].

The reconstruction step is to back-project for each $(x, y)$ the value of the projection at $\theta$ angle in which $(x, y)$ is crossed by the ray of projection.

$$i = x\cos(\theta) + y\sin(\theta) \tag{4}$$

$$f_\theta'(x, y) = p_\theta(i) \tag{5}$$

The back-projection of all projections can be given as

$$f'(x, y) = \int_0^\Pi p_\theta(i)d\theta \tag{6}$$

By analogy, in discrete case the back-projection is computed such that

$$f'(x, y) = \sum_{\theta=0}^{\Pi} p(i, \theta) \tag{7}$$

With $f'$ is the reconstructed object.

In overall, the image reconstruction in tomography can be summarized into two main steps:

1. Produce the projections from the image. The projections are collected as sinogram mode, see Fig. 2.
2. From these projections (sinogram) we reconstruct the image [5], see Fig. 3.

Several methods for image reconstruction are studied in CT. These methods can be divided into two main categories: analytical and iterative methods. The next subsection gives an overview on some well-known standard methods for image reconstruction in tomography.
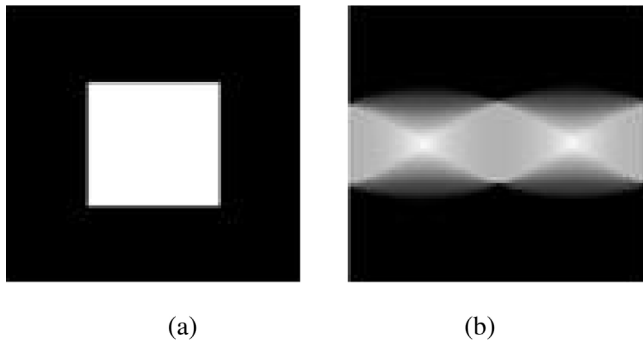
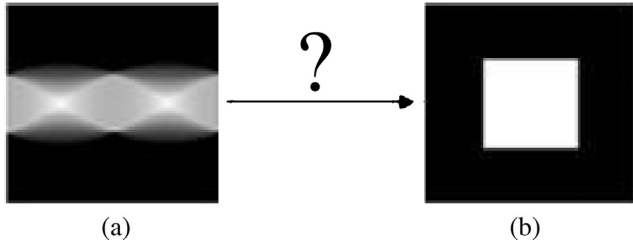**Fig. 2.** Example of an object (a) and its sinogram (b).



**Fig. 3.** Illustration of the principle of reconstruction: from sinogram, we try to reconstruct the object.

### 2.2. Standards methods

*This section describes briefly the two main categories of standard methods of image reconstruction from projections.*

#### 2.2.1. Analytical methods

The analytical methods are based on continuous modeling; it consists of inverse measurement equations. Among the analytical methods, we cite the simple back projection method that is just reversing the projection operation which gave rise to the data. The Fourier transformation method that estimates the distribution by inverting Fourier transform theorem. The back-projection (BPF) method where the projection data are first back-projected, filtered in Fourier space. Finally, the filtered back-projection (FBP) method where projection data are first filtered and then back projected [31,32]. Filtered back-projection (FBP) [6] is the most used analytical method, and in general, analytical methods are fast but the quality of reconstruction is largely disputed. The iterative methods have been introduced to improve the quality of reconstructed images.

#### 2.2.2. Iterative methods

The iterative methods aim to find a solution $f$ that minimizes the error between $p$ and $p'$ [8,7,9,33].

$$p' = M \cdot f \tag{8}$$

With $p$ is the measured projections. $p'$ is the estimated one. $M$ is the coefficient (system) matrix. It represents the probability of contribution of each pixel in each projection. The iterative method uses a specific error correction to minimize error between $p$ and $p'$.

The iterative methods have been introduced to improve the quality of reconstructed images. Among these methods, we can find SIRT method or ordered subset expectation maximization (OSEM) [33]. In general, iterative methods provide better quality images than analytical methods. However, these methods need heavy computing power, the noises increase with the number of iterations and after a number of iterations the solution starts to diverge significantly.

### 2.3. Others methods

As already said in the introduction, there are only few meta-heuristics based methods for image reconstruction in tomography such as: the genetic and fly algorithms for image reconstruction [23,17,13,14,16]. The problem is still open, because there is no exact solution for this problem and the quality of the reconstructed images could be still enhanced.

In the next section, we propose two meta-heuristics for image reconstruction from projections. The first is a harmony search (HS) and the second is a hybrid HS with a local search method to enhance the quality of reconstructed images with low resolution. The proposed methods are compared with the most used analytical method in CT which is FBP and the iterative SIRT method.

## 3. Proposed approaches

In this section, we propose two methods for image reconstruction in tomography. The first is based on the recent harmony search (HS) meta-heuristic. The second is a combination of HS and the local search method (LS) [18]. In following we start with the principles of HS. Then we give the two proposed methods for image reconstruction in tomography.

### 3.1. Classical definition of harmony search meta-heuristic

Geem et al. [34] have developed in 2001, a new algorithm based on the improvisation process of musicians which want to find the perfect harmony in a musical orchestra where each musician plays a musical note seeking a better harmony. Especially those who never played together before, they search rapidly to improve their individual contributions in order to find the best harmony [34]. This algorithm is called "harmony search HS". This method was applied in some fields [35–37] but not yet in tomographic reconstruction. The six main steps of the harmony search method are given as follows.

*Step 1.* *The initialization of the problem and algorithm parameters*
  The first step is to initialize the algorithm parameters. We note that the optimization problem is to optimize a certain objective function $R(x)$ subject to $x_i \in M$, $i = 1, 2, 3, \ldots, N$. $x$ is a possible solution to the problem, it is the set of decision variables (called also solution vector); $N$ is the number of decision variables; $M$ is a list of sets, each set $M_i$ containing the possible values of a variable $x_i$ within its bounds.

*Step 2.* *The initialization of the harmony memory (HM)*
  HM is the set of solutions (harmonies). Each solution is a row vector of $N$ numbers $x_i$. Thus, HM can be noted as a matrix, where the rows contains harmonies and the number of rows are bounded by the harmony memory size (HMS). Thus, a column within this matrix contains all estimated solution values for one variable $x_i$.

$$HM = \begin{pmatrix} x_1^1 & x_2^1 & \cdots & x_N^1 \\ x_1^2 & x_2^2 & \cdots & x_N^2 \\ \vdots & \vdots & \vdots & \vdots \\ x_1^{HMS} & x_2^{HMS} & \cdots & x_N^{HMS} \end{pmatrix}$$

Once the problem is specified and the HM is initialized, the parameters have to be specified also. These HS parameters are:

- **HMS**: which is the harmony memory size that represents the number of solution vectors in the harmony memory (HM).
- **HMCR**: is the harmony memory considering rate, $HMCR \in [0, 1]$.
- **PAR**: is the pitch adjusting rate, $PAR \in [0, 1]$.
- **NI**: is the number of improvisations or stopping criterion.

Step 3. *The objective function computation*

The objective function permits to measure the quality of the generated solutions. The definition of the objective function depends to the considered optimization problem.

Step 4. *The improvisation of a new harmony from the HM*

A new HM vector $X' = x'_1, x'_2, \ldots, x'_N$ is produced based on three rules: (1) memory consideration, (2) random selection and (3) pitch adjustment. The harmony memory considering rate, $HMCR \in [0, 1]$ is the probability of choosing a value from the $i$-th column within HM, while the $(1 - HMCR)$ is the probability of randomly selecting one value of the possible range of values.

$$x'_i = \begin{cases} x_i \in \{x_i^1, x_i^2, \ldots, x_i^{HMS}\} & w.p. \quad HMCR \\ x_i^L + rand() \cdot (x_i^U - x_i^L) & w.p. \quad (1 - HMCR) \end{cases} \quad (9)$$

With $L$ and $U$ the lower and upper bounds for the given problem. rand() is a uniform distribution random number between 0 and 1.

The value of each decision variable obtained by the memory consideration is examined to determine whether it should be pitch-adjusted. Pitch adjustment means changing the value of $x'_i$. This operation uses the $PAR$ parameter. $PAR$ is the probability of choosing a neighboring solution $x'_i = x_i \pm rand() \cdot BW$. Where $BW$ is a random number in the feasible space between the lower and upper bound values ($L$ and $U$), [38–40]. The value of $(1 - PAR)$ sets the rate of performing nothing.

$$x'_i = \begin{cases} x_i \pm rand() \cdot BW & w.p. \quad PAR \\ x'_i & w.p. \quad (1 - PAR) \end{cases} \quad (10)$$

Step 5. *Update of the HM*

The new generated harmony vector is inserted into HM when it is better than the worst harmony in the HM. The worst harmony is then removed from the HM. The update of HS depends highly on the search experience. The quality of a harmony is measured by using the objective function.

Step 6. *Repeat Steps 3 and 4 until satisfaction of stopping criterion*

The Steps 3 and 4 are repeated until the maximum number of improvisations is satisfied.

### 3.2. Adaptation of HS to our problem

The problem of image reconstruction from projections is considered as an optimization problem. It aims to improve the quality of reconstructed images with low resolution. We attempt to find the best image by minimizing a certain objective function. In our case, the objective function measures the distance between estimated and measured projections.

*In the following, we adapt HS to the problem of image reconstruction from projections. HS is an iterative method aiming to minimize the distance between estimated and measured projections.*

#### 3.2.1. Creation of the initial population called HM

The HS method starts with an initial population HM generated randomly. In our case, the initial solution represents the initial reconstruction of the image from the projections using a standard analytical method.

#### 3.2.2. Generation of new harmonies

The generation of new harmonies at each iteration called also neighborhood solutions generation permits to explore the search space and locate new solutions. We produced three different new solutions as follows.

1. If $HMCR_i < HMCR$ then a new solution is produced from the HM, for each new harmony, we choose the value of the solution $S_t(t \in [1, HMS]$, randomly chosen from HM.

$$S' = S_c \cdot S_q \quad (11)$$

With $S'$ the first neighborhood solution (image). $S_c$ the current solution. $S_q$ the produced solution from estimated projections using a simple back-projection. These estimated projections are produced by estimating the quotient from measured projections and estimated one, from the factor of correction used in [41]. We note that $HMCR$ is the harmony memory considering rate specified at the beginning of HS. $HMCR_i$ is a probability computed at each iteration of HS process.

2. If $PAR_i < PAR$ then we produce from the value of the current solution $S_c$ three new neighbors solutions, such as (11) and (12).

$$S'' = S_c + S_d \quad (12)$$

With $S''$ the second neighborhood solution. $S_c$ the current solution. $S_d$ the produced solution from estimated projections. These estimated projections are produced by estimating the distance between measured projections and estimated one, from the factor of correction used in [7]. We note that $PAR$ is the Pitch Adjusting Rate fixed when HS is started. $PAR_i$ is a probability computed at each iteration of HS method.

3. The third neighborhood solution $S'''$ is given by a simple move. The move is an operator that represents a modification applied on a candidate solution $S_c$ to produce new ones $S'''$. In our case the modification is the direct change of grayscale value of one or some pixels by another value.

#### 3.2.3. The objective function

The objective function permits to measure the quality of a solution $x$. In our case, the objective function is the distance between all measured projections (sinogram) and the estimated projections from the current solution $x$.

City block distance [42], is used because it gives a high quality of precision and it is a fast method.

The projection is recorded into sinogram $H(s,\theta)$. We compute the sum of the distances ($R$) between each estimated projection of changed point that recorded into sinogram $H_c(s,\theta)$ and each measured projection for the same angle $\theta$ from the same point recorded into sinogram $H_m(s,\theta)$, such (13):

$$R = \sum_{s,\theta} |H_c(s, \theta) - H_m(s, \theta)| \quad (13)$$

#### 3.2.4. Update HM

From the produced solutions, the best solution which has the smallest distance is chosen. This solution is added in the HM and the historical solution with the maximum value (the worst one) of distance is removed.

#### 3.2.5. NI

The algorithm stops when the convergence criteria referred to the computed objective function $R$ converge to a fixed value $V$ or if the time bound is elapsed. Otherwise the HS is applied to all points (pixels) of the image.

### 3.3. The LS algorithm

Local search is an iterative meta-heuristic that moves from one solution to the next one by applying local changes until the optimal solution is found or the time bound is elapsed [18]. The adapted LS is based on the following steps.

- **Step0**: *Initialization*: produce an initial solution.
- **Step2**: each point of the solution is changed with different grayscale values, projections data are estimated for the all modifications.
- **Step3**: *Objective function*: this function estimates the distance between current projection and measured one for a specific angle $\theta$ and the same point that contribute in this projection.

  For each point that contributes in each projection, we compute this function and proceed to a selection of the best new solutions.
- **Step4**: *Selection*: we select the solution having the minimum distance value between the current estimated projection and the measured one.
- **Step5**: *Stopping condition*: the algorithm is stopped when the current solution converge to the previous one. Otherwise the local search algorithm is applied for all points of the images for all measured projections.

### 3.4. Hybrid HS

We combine HS and LS methods to enhance further the performance of our method for reconstructing images with low resolution. First we call HS to reconstruct an image and estimate the reconstruction quality. When HS fails to find a good solution and there is no satisfactory reconstruction, we call LS algorithm to enhance the quality of solution produced initially by HS. The overall method is given as follows:

1. Call HS algorithm.
2. if $R > V$ and $T < T_s$ then call LS algorithm.

  Where $T$ is the image resolution. The aim is to apply the hybrid method only for images with low resolution. $T_s$ represents the maximum image resolution (number of unknowns), which is fixed empirically to 2500. $R$ is the objective function already given in Section 3.2.3. The LS method is called when HS fails to improve significantly the quality of reconstructed images.

## 4. Experimental study

The proposed methods are implemented on machine and compared with some well-known methods for image reconstruction. The aim of this section is to give some results and to show the effectiveness of the proposed methods for image reconstruction in tomography.

### 4.1. The used machine

All experiments are run on a personal computer with Intel(R) Core(TM), 2.4GHZ 2.4 i7 CPU GHZ with 6.00GB of RAM under Windows 7 system. The codes are implemented in MATLAB.

### 4.2. Parameter tuning

The adjustment of the parameter of the proposed approaches is fixed by an empirical study. The HS parameters are: $Z = 4$, $V = 0.05$ and CPU time for $HS = 500$ s.

**Table 1**
The gap and the computation time needed for each reconstruction from Fig. 4 using HS and FBP methods.

| Image test | Size | HS | | FBP | |
|---|---|---|---|---|---|
| | | Gap | Time (s) | Gap | Time (s) |
| Image test 01 | $10 \times 10$ | 0 | 0.97 | 0.27 | **0.175** |
| Image test 02 | $20 \times 20$ | 0 | 1.36 | 0.82 | **0.14** |
| Image test 03 | $10 \times 10$ | 0 | 0.30 | 0.25 | **0.084** |
| Image test 04 | $10 \times 10$ | 0 | 0.3 | 0.28 | **0.085** |
| Image test 05 | $20 \times 20$ | 0 | 0.19 | 0.05 | **0.10** |
| Image test 06 | $30 \times 30$ | 0 | 1.58 | 1.05 | **0.10** |

**Table 2**
Comparison of reconstructed images from Fig. 4 by using HS and FBP methods.

| Image test | HS | FBP |
|---|---|---|
| | PSNR | |
| Image test 01 | $\infty$ | 59.1709 |
| Image test 02 | $\infty$ | 62.3217 |
| Image test 03 | $\infty$ | 64.7573 |
| Image test 04 | $\infty$ | 61.1984 |
| Image test 05 | $\infty$ | 61.1059 |
| Image test 06 | $\infty$ | 66.7509 |

### 4.3. Numerical results

The aim of this section is to evaluate the proposed approaches on some datasets. We developed synthetic images with low resolution on which we applied HS and hybrid HS algorithms.

The proposed methods are also validated on the famous Shepp–Logan and Hoffman models. The results obtained from the series of tests are presented in this section.

The quality of the image reconstruction is measured by computing the peak signal to noise ratio (PSNR) between the reconstructed image and the original one [43,44]. PSNR is an expression for the dispersion between the reconstructed image and the original one as given in the following formula.

$$PSNR = 10lg\left(\frac{d^2}{MSE}\right) \tag{14}$$

$$MSE = \frac{1}{mn}\sum_{i=0}^{m-1}\sum_{j=0}^{n-1}\|I_0(i,j) - I_r(i,j)\|^2 \tag{15}$$

With $d$ is the maximum possible pixel value of the image. $I_0$: is the original image. $I_r$: is the reconstructed image. For MSE = 0, PSNR becomes infinite.

We computed also, the gap that represents the error between each reconstructed image with the original one. For this, Manhattan distance is computed as given in the following formula.

$$gap = \sum_{i=0}^{m-1}\sum_{j=0}^{n-1}I_0(i,j) - I_r(i,j) \tag{16}$$

$I_0$: is the original image. $I_r$: is the reconstructed image.

### 4.4. Test1: results on six synthetic images

Fig. 4 compares the performance of HS and FBP methods on six synthetic images. We give also the original image to shows clearly the effectiveness of HS compared to FBP.

The obtained PSNR, the gap and the CPU time in second needed for the reconstruction process by each method are given in this section. Table 1 gives a quantitative comparison using the gap metric while Table 2 gives a quantitative comparison based on PSNR metric. The tests are done on some images from Fig. 4.
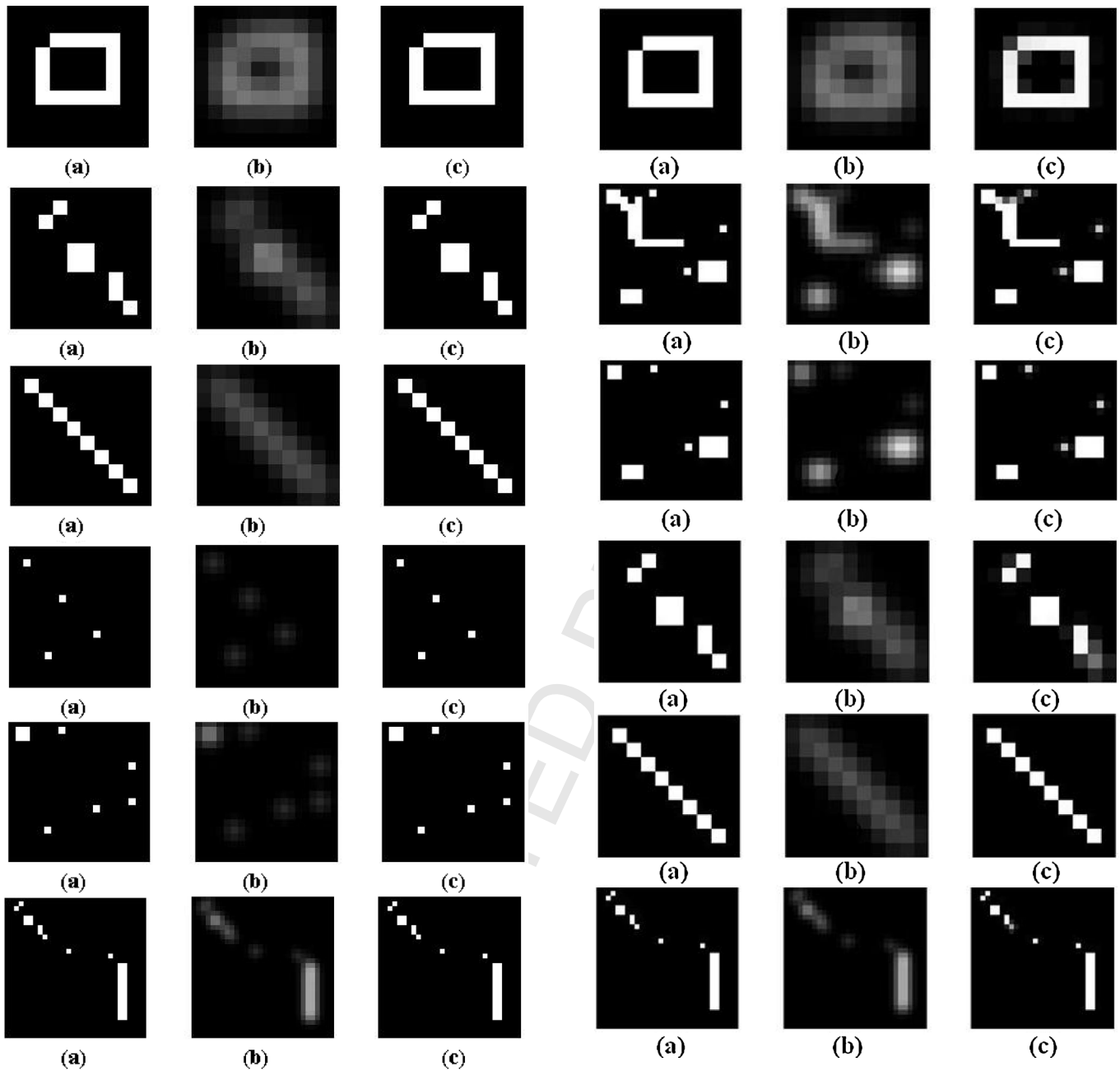
**Fig. 4.** Example of reconstructed images. (a) Original image. (b) Reconstructed image by FBP method. (c) Reconstructed image by HS method.



**Fig. 5.** Example of the worst reconstruction with HS in 10 runs. (a) Original image. (b) Reconstructed image by FBP method. (c) Reconstructed image by HS method.

We can see from Table 2 that HS succeeds in giving a high quality of reconstructed images. Indeed, the PSNR values of reconstructed images by HS method are slightly better than PSNR of FBP reconstruction. The search process in HS is not a time consuming compared to the reconstruction process in FBP method, as shown in Table 1.

### 4.5. Test2: the worst solution found

In this test, we study the quality of reconstructed images test of Fig. 5. We produce the worst solution found by the proposed method during 10 runs and we compare this solution with the one created by FBP.

Fig. 5 shows clearly that HS method succeeds in providing good quality of reconstructed images.

The numerical results in Table 3 indicate that the PSNR values of the produced solutions, for all tests, are still better than the PSNR values of the reconstructed image by FBP method.

### 4.6. Test3: importance of the hybrid method

Test3 gives the results obtained for images of Fig. 6. Here the aim is to show the importance of the hybrid method when the HS method lunched alone fails to give a good image reconstruction. We cite the cases of *Image test 02* and *Image test 03* from Fig. 6. Here the hybrid method succeeds to improve the quality of image reconstruction. The hybrid method finds better solutions than both HS and FBP.

**Table 3**
Comparison of reconstructed images from Fig. 5 by using FBP and HS methods.

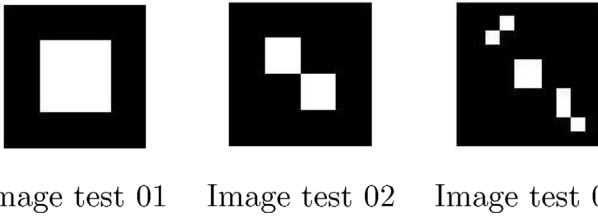| Image test | HS | FBP |
|---|---|---|
| | PSNR | |
| Image test 01 | **74.8387** | 59.1709 |
| Image test 02 | **76.5673** | 62.3217 |
| Image test 03 | **81.0638** | 64.7573 |
| Image test 04 | **71.0369** | 61.1984 |
| Image test 05 | **104.0399** | 61.1059 |
| Image test 06 | **84.2095** | 66.7509 |



**Fig. 6.** Images test for *test 03*.

### 4.6.1. Comparison between HS and FBP

We depicted in Fig. 7 the reconstructed image by both FBP and HS methods. We can see that HS method enhances the quality of reconstructed images for *Images test 01* and *Image test 03* from Fig. 6.

We can see from Table 4 that the quality of the reconstructed *Image test 01* and *Image test 03* of Fig. 6 by using HS method is better than the quality of FBP reconstruction in term of gap point of view. Nonetheless the gap value of reconstructed *Image test 02* by using FBP method is weaker than the gap value of reconstructed image by using HS. Therefore, HS fails to improve the quality of reconstructed Image test 02.
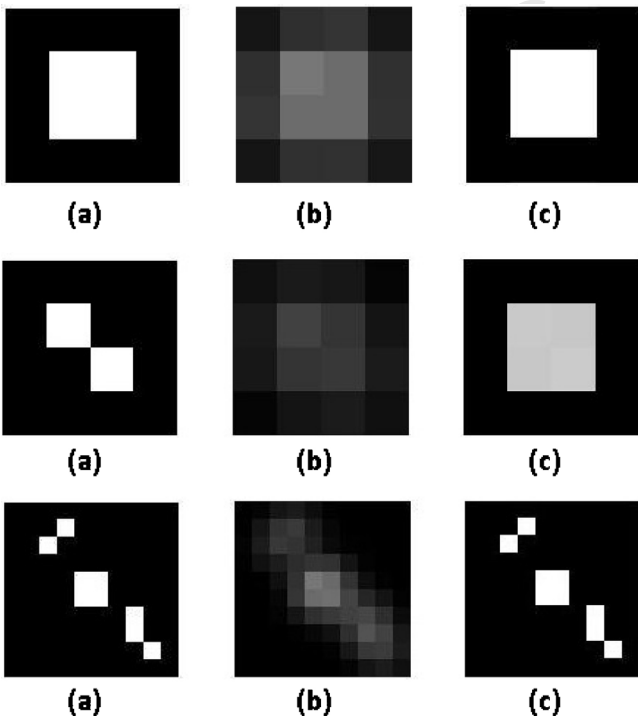


**Fig. 7.** Example of reconstructed images from Fig. 6. (a) Original image. (b) Reconstructed image by FBP method. (c) Reconstructed image by HS method.

**Table 4**
The gap and the computation time needed for each reconstruction of images from Fig. 7 by using HS and FBP methods.

| Image test | HS | | FBP | |
|---|---|---|---|---|
| | Gap | Time (s) | Gap | Time (s) |
| Image test 01 | **0.01** | 0.046 | 0.38 | 0.002 |
| Image test 02 | **0.19** | 0.05 | 0.18 | 0.002 |
| Image test 03 | **0** | 0.05 | 0.23 | 0.002 |

**Table 5**
The gap and the computation time needed for each reconstruction of images (c) and (d) from Fig. 8 using the HS method.

| Image test | HS | | | |
|---|---|---|---|---|
| | Gap (c) | Gap (d) | Time (c) | Time (d) |
| Image test 01 | 0.15 | **0.01** | 0.012 | 0.046 |
| Image test 02 | **0.19** | 0.19 | 0.045 | 0.07 |
| Image test 03 | 0.09 | **0** | 0.31 | 0.05 |

### 4.6.2. The best versus the worst produced solutions

In this section, we study the quality of the image reconstruction for each image test from Fig. 6 by displaying the best and the worst solutions obtained by using the same proposed method. Fig. 8 gives an example of the best and the worst reconstructed images produced by HS method.

According to the results from Table 5 and Fig. 8, we can say that HS method when lunched alone improves the quality of reconstructed images for *Image test 01* and *Image test 03*. The gap of both reconstructed images is better than the gap of reconstructed image by using FBP. Unlike the *Image test 02* where the gap of the two produced solutions could be rounded to the gap value of FBP reconstruction.

The worst and the best solutions shown in Fig. 8 indicate that HS method cannot reach the global optimum on every run. HS sometimes loses its way at a local optimum for a few tests, as in *Image test 01* from Fig. 6.

### 4.6.3. Comparative study between HS, FBP and LS methods

As given in Tables 1 and 6, the gap of reconstructed images by HS is mostly better than the gap of reconstructed image using FBP.

Let us focus on *Image test 01* from Fig. 6, the worst gap concerns image (c) from Table 5, the gap = 0.15 which is still better than the gap of reconstructed image by FBP method (gap = 0.38), which means that the quality of reconstructed image by HS method is much better than reconstructed image by FBP method.

The gap concerning the *Image test 02* is the same for FBP and HS reconstruction, which means no improvement.

To improve the quality of reconstructed image, we combined HS and LS meta-heuristics. The hybrid algorithm succeeds to improve the quality of reconstructed image.

For *Image test 03*, the quality of the produced image by using HS method is slightly better than the reconstructed image by using FBP method as shown in both Table 4 and Fig. 7, we do not need hybridization with LS method.

**Table 6**
The gap and the computation time needed for each reconstruction of images from Fig. 9 using HS and LS methods.

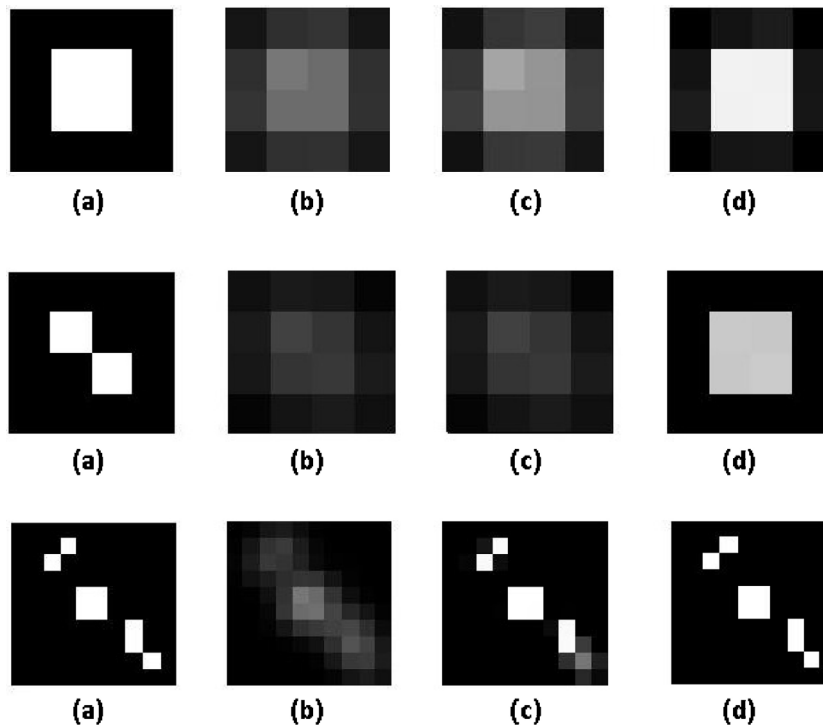| Image test | HS | | LS | |
|---|---|---|---|---|
| | Gap | Time (s) | Gap | Time (s) |
| Image test 01 | 0.01 | 0.046 | **0** | 0.55 |
| Image test 02 | 0.19 | 0.07 | **0** | 1.02 |
| Image test 03 | **0** | 0.05 | **0** | 9.71 |

**Fig. 8.** Example of the worst and the best obtained images by HS method. (a) Original image. (b) Reconstructed image by FBP method. (c) The worst obtained image by HS method. (d) The best obtained image by HS method.

Table 6 and Fig. 9 show clearly that LS method is better for reconstruction than HS method. The gap of reconstructed images by the LS method is better than the gap of reconstructed images by HS method. However, as shown in Table 6, the computation time of the HS is largely better than the computation time of LS method, which is an important parameter.

We note that the gap of *Image test 03* is the same for the two methods. However, the number of the misplaced pixels (NMP) of reconstructed *Image test 03* using HS method is NMP = 0 while NMP = 4 when it is reconstructed by LS method.

The gap of *Image test 01* when using HS method (gap = 0.01) is close to 0 values and the time of computation is smaller than time
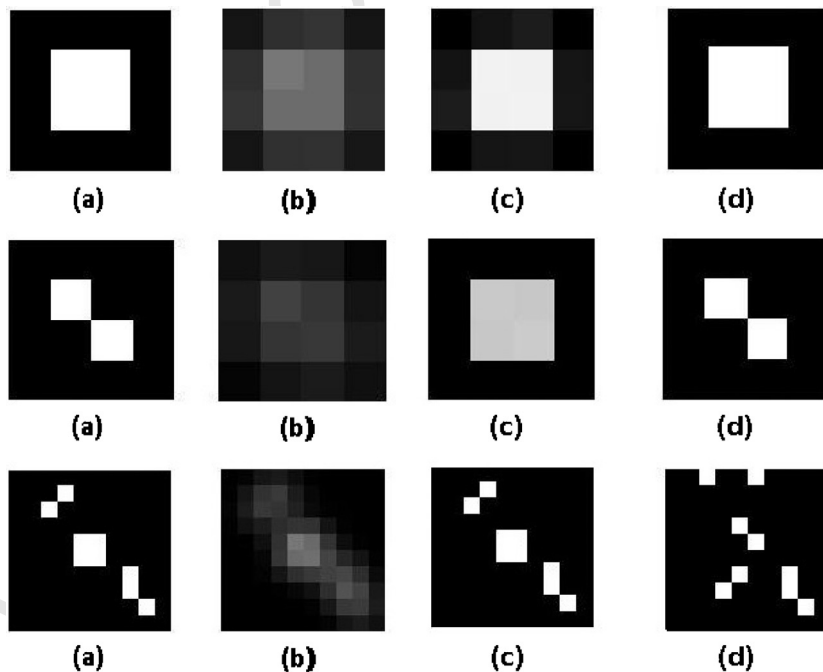


**Fig. 9.** Example of reconstructed images from Fig. 7. (a) Original image. (b) Reconstructed image by FBP method. (c) Reconstructed image by HS method. (d) Reconstructed image by LS method.
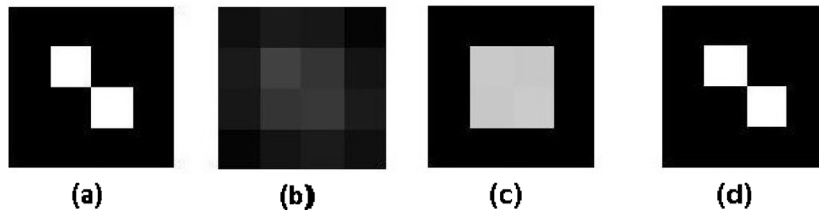
**Fig. 10.** Example of reconstructed images using a hybrid HS. (a) Original image. (b) Reconstructed image by FBP method. (c) Reconstructed image by HS method. (d) Reconstructed image by HS/LS method.

**Table 7**
The gap and the computation time needed for each reconstruction of images from Fig. 10 using the HS and hybrid HS with LS methods.

| Image test | HS | | HS/LS | |
|---|---|---|---|---|
| | Gap | Time (s) | Gap | Time (s) |
| Image test 02 | 0.19 | 0.07 | **0** | 1.21 |

calculation of LS method. Accordingly, HS approach is better than the LS method.

### 4.6.4. Hybridization between HS and LS methods

The gap concerning the *Image test 02* is better with LS method, and for these reasons we apply a hybrid HS to reconstruct this image. The obtained results are shown in Fig. 10 (Table 7).

### 4.7. Further comparison with FBP method

The aim of this section is to show the performance of HS method compared to FBP method by using Shepp–Logan model, noisy projections and the ANOVA statistical test.

### 4.7.1. Test4: HS versus FBP on Shepp–Logan model

Test4 presents the HS reconstruction results applied on a famous Shepp–Logan model, see Fig. 11. We compare the reconstructed image by HS with the reconstructed one using FBP method. The values cited in Fig. 11 show the peak signal to noise ratio (PSNR) of each reconstructed image by HS and FBP methods. The PSNR resulting for the FBP and HS is given in Fig. 11. The value of PSNR of the reconstructed image using our method is better than the value of PSNR of the reconstructed image by FBP. According to the numerical results, we can say that HS method is able to find high quality solutions.

### 4.7.2. Test5: the effectiveness of HS when introducing noises

Test5 describes the efficiency of our method when introducing noises. Fig. 12 shows the results obtained by using our approach and FBP method on a famous Shepp–Logan model with noises. We compare the reconstructed image by our method with the reconstructed one with FBP method. The value of PSNR of the



PSNR= **65.7**    PSNR= **67.7**

**Fig. 12.** HS reconstruction, including noises. (a) Original model. (b) Reconstructed image by FBP method. (c) Reconstructed image by HS method.

reconstructed image by using HS method is better than the value of PSNR of the reconstructed image by using FBP method. We deduce that HS is able to find good quality solutions in spite the introduction of noises.

### 4.7.3. ANOVA statistical analysis: test 01

Analysis of variance (ANOVA) is a statistical tool used to analyze the differences between groups on some variable. ANOVA is available for both score data and ranking data.

The purpose of one-way ANOVA is to determine whether different groups of an independent variable have different effects on the response variable. The purpose of one-way ANOVA is to determine whether data from several groups (levels) of a factor have a common mean. In our test, we want to determine if our method improves the quality of reconstructed images more than the FBP standard method. In this case, the independent variable is PSNR values for a set of reconstructed images by each FBP and HS method (Table 8).

In this section, we draw the table that shows the value of the *F*-statistic and *p*-value. The boxplot of the quality of reconstruction between FBP and HS reconstruction is given in Fig. 13. The ANOVA results of the image quality measures (out of 20 tested) in each image obtained from FBP reconstruction and our proposed method is given in Table 9 and Fig. 13.

**Table 8**
The one-way ANOVA test1: quality of reconstruction between FBP and HS reconstruction. Only for variance source between groups (columns).

| SS | df | MS | F-statistic | p-Value |
|---|---|---|---|---|
| $2.04^{e+006}$ | 1 | 2,038,400.3 | 18.3 | **0.0001** |

**Table 9**
The one-way ANOVA test: quality of reconstruction between SIRT and HS reconstruction.

| SS | df | MS | F-statistic | p-Value |
|---|---|---|---|---|
| 2728 | 1 | 2728.02 | 12.28 | **0.0012** |



PSNR= 66.15    PSNR= **72.23**

**Fig. 11.** Shepp and Logan model for Test4. (a) Original model. (b) Reconstructed image by FBP method. (c) Reconstructed image by HS method.
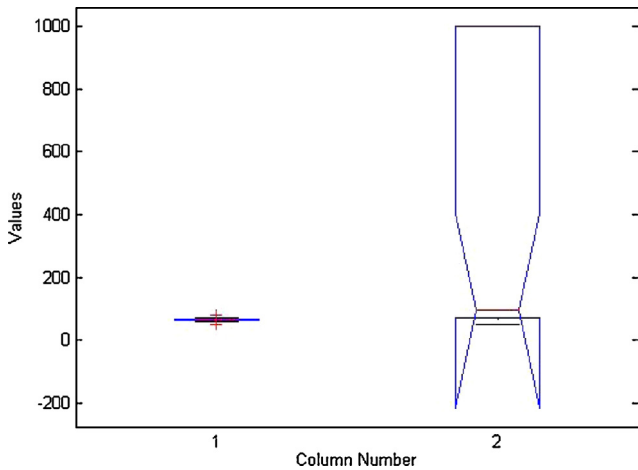
**Fig. 13.** Boxplot of one-way ANOVA: The quality of reconstruction between FBP and HS reconstruction. (1) FBP reconstruction. (2) HS method.



(a)                    (b)                    (c)

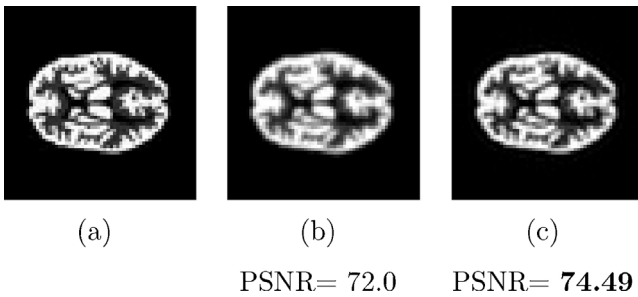PSNR= 72.0          PSNR= **74.49**

**Fig. 14.** HS reconstruction from noiseless projections compared with SIRT. (a) Original model. (b) Reconstructed image by SIRT method. (c) Reconstructed image by HS method.



(a)                    (b)                    (c)

PSNR= 71.93          PSNR= **75.64**

**Fig. 15.** HS reconstruction from noisy projections compared with SIRT. (a) Original model. (b) Reconstructed image by SIRT method. (c) Reconstructed image by HS method.



**Fig. 16.** ANOVA boxplots: the quality of reconstruction between SIRT and HS reconstruction. (1) SIRT reconstruction. (2) HS method. (For interpretation of the references to color in text near the reference citation, the reader is referred to the web version of this article.)                                    **Q6**

Table 9 describes the ANOVA table. The column *SS* is the Sum of squares. The column *df* represents the degree of freedom. The column *MS* is the mean square.

The *p*-value from the ANOVA table is around 0.0001. This result indicates that the values of column number 2, which represents the PSNR values of reconstructed images produced by HS method, are significantly different from the values of column number 1, which represents the PSNR values of images produced by FBP reconstruction. The Fig. 13 shows that PSNR values of reconstructed images using our method have a wider dispersion of the data. The boxplot confirms graphically that the quality of reconstructed images using our method is statistically better than those reconstructed by using FBP method.

### 4.8. Further comparison with SIRT method

The aim of this section is to show the performance of the HS method compared to the SIRT method. We validate the two methods on the famous Hoffman model. We consider noisy projections and we give the ANOVA statistical test.

#### 4.8.1. Test6: comparison between SIRT and HS without noise consideration

We present in Fig. 14 the performance of reconstruction obtained by HS method, SIRT method and the original image without introducing noise. We can see that HS succeeds in giving a high quality of reconstructed images. Indeed, the PSNR values of reconstructed images by HS method are better than PSNR of the reconstructed one by using SIRT method.

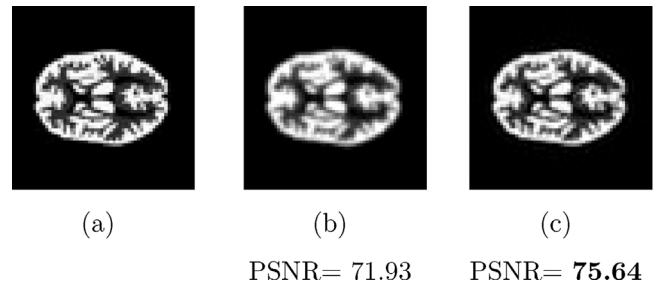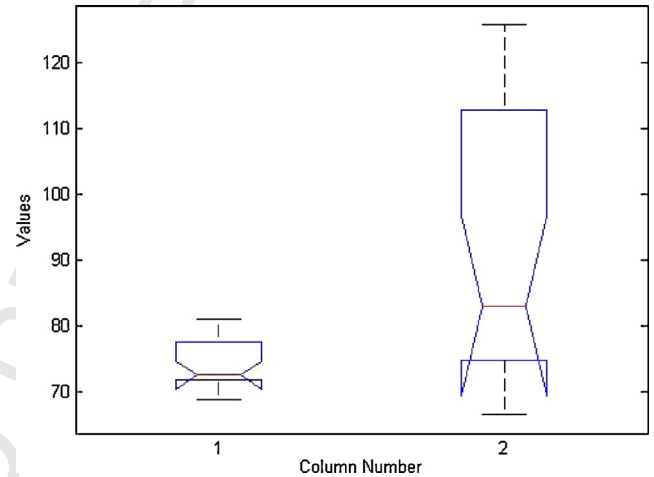The PSNR value is obtained from a random running of HS method. Because, as proven previously HS succeeds largely to improve the reconstruction, at least for 10 runs even that is a non-deterministic method.

#### 4.8.2. Test7: comparison between SIRT and HS with noise consideration

Fig. 15 gives the performance of reconstruction obtained by HS method, SIRT method and the original one introducing Poisson noises. The value of PSNR of the reconstructed image using HS method is better than the value of PSNR of the reconstructed image by using SIRT method, which means that our method succeeds in finding high quality images even noises are introduced.

#### 4.8.3. ANOVA statistical analysis: test 02

This section tries to determine whether the proposed method improves the quality of reconstructed images more than the SIRT standard method. In this test, the independent variable is the quality of reconstruction using the methods of reconstruction (SIRT and HS).

The ANOVA table shows the value of the *F*-statistic and *p*-value. The boxplot of two different groups is given in Fig. 16. The ANOVA results of the image quality measures (out of 20 tested) in each image obtained from SIRT reconstruction and our proposed method is given in Table 9 and Fig. 16. Fig. 16 shows boxplots of two different groups (columns).

The column number 1 represents the PSNR values of the 20 reconstructed images using SIRT method. The column number 2 represents the PSNR values of the 20 reconstructed images using HS method.
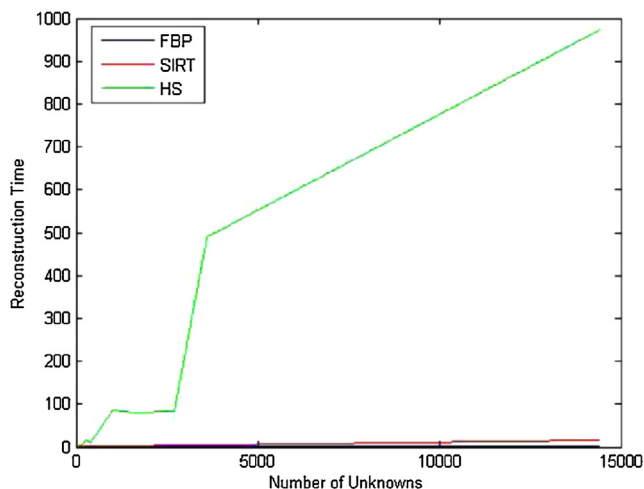
**Fig. 17.** The reconstruction time (s) needed by FBP, SIRT and HS methods.

The *p*-value from the ANOVA table is around 0.0012 which indicates that the PSNR values between groups are significantly different. The boxplot shows that PSNR values of reconstructed images using our method have a wider dispersion of the data. The boxplot confirms this result graphically. We can see that the difference between the column means (mean is given in red line) is highly significant. The boxplot and the *p*-value confirm that the quality of reconstructed images using harmony search meta-heuristic is statistically better than the quality of reconstructed images by using SIRT method.

### 4.9. The reconstruction time

We computed the running time consumed by the different methods (FBP, SIRT and HS) for image reconstruction. We draw the curves in Fig. 17 that represent the number of unknowns (images resolution) versus time taken for reconstruction.

According to the curves, the time of computation of the reconstructed images by using HS is higher than the time needed by SIRT or FBP method. The curve of HS computation time increase greatly with the increase in required resolution and hence parallelism of the algorithm becomes necessary in such case.

### 4.10. Discussion

As shown in Fig. 4, our method based on HS improves the quality of reconstructed images compared to FBP method. Indeed, all objects, even different, were reconstructed with high quality of reconstruction.

Added to this, Image test 01 and Image test 02 from Fig. 6, was used to perform our method for some reconstructed images with lower quality than those compared to others. The improvement consists of hybridization between HS method with LS algorithm. As shown, the hybrid method succeeds to perform quality of some reconstructed images by the HS method with low quality.

The numerical results, confirm that our method improves the quality of reconstruction compared to FBP approach for images with small resolution, even noises are introduced. Indeed, the gap of all reconstructed images with FBP method >0 unlike our HS method, as we see in Tables 1 and 4. The values also of PSNR confirm that our method is more efficient than FBP method. However, it is more time consuming than FBP method which is the fastest method of reconstruction.

HS was also applied to reconstruct some famous model as Shepp–Logan and Hoffman model. The obtained quantitative and qualitative results prove the efficiency of HS for reconstruction from projections even noises are introduced.

The obtained results using statistical ANOVA test to compare our method with the analytical FBP and the iterative SIRT methods demonstrate that the difference in performance is statistically significant. Nonetheless HS reconstruction time is higher than computation time needed by SIRT or FBP method.

## 5. Conclusion

In this paper, we proposed two meta-heuristics for image reconstruction in tomography. The first is harmony search algorithm (HS) for the problem of image reconstruction. The second is hybrid HS with LS algorithm for the considered problem. The two proposed methods are evaluated on some images and compared to both the analytical FBP and the iterative SIRT methods. The obtained results are competitive and demonstrate the benefit of our methods. The results prove the applicability and the efficiency of the developed approaches. Further, the hybrid HS with LS is able to find good results compared to the other considered methods. We plan to add diversification to prevent hybrid HS losing its way at local optimum and also include noises correction. Further refinements will introduce the parallelism under GPU to reduce computation time.

## References

[1] C. Mou, L. Pen, D. Yao, D. Xiao, Image reconstruction using a genetic algorithm for electrical capacitance tomography, Tsinghua Sci. Technol. 10 (5) (2005) 587–592.

[2] R.Z. Liu, Q.W. Tian, S.J. Yu, H. Chen, X.L. Min, Triangular grid sonic computerized tomography for structural concrete, Prog. Geophys. 29 (4) (2014) 1907, http://dx.doi.org/10.6038/pg20140458.

[3] R. Gordon, Reconstruction from projections in medicine and astronomy, in: C. Van Schooneveld (Ed.), Image Formation from Coherence Functions in Astronomy, vol. 76 of Astrophysics and Space Science Library, Springer, Netherlands, 1979, pp. 317–325, http://dx.doi.of: Image reconstruction from projections. San Francisco: Academic Press, 1980. URL http://opac.inria.fr/record=b1132441).

[4] N. Kumar, T. Srivastava, Image reconstruction from projection under periodicity constraints using genetic algorithm, in: S. Ranka, A. Banerjee, K.K. Biswas, S. Dua, P. Mishra, R. Moona, S.-H. Poon, C.-L. Wang (Eds.), IC3 (1), vol. 94 of Communications in Computer and Information Science, Springer, 2010, pp. 76–83, URL http:// dblp. uni- trier. de/ db/ conf/ ic3/ ic3- 2010- 1. html#KumarS10.

[5] G.T. Herman, Fundamentals of computerized tomography: image reconstruction from projections, in: Advances in Pattern Recognition, Springer, Dordrecht, New York, 2009 (rev. ed. of: Image reconstruction from projections. San Francisco: Academic Press, 1980. URL http://opac.inria.fr/record=b1132441).

[6] J. Fessler, Analytical Tomographic Image Reconstruction Methods, 2009 (Chapter 3).

[7] P. Gilbert, Iterative methods for the three-dimensional reconstruction of an object from projections, J. Theoret. Biol. 36 (1) (1972) 105–117, http://dx.doi.org/10.1016/0022-5193(72)90180-4.

[8] L.A. Shepp, Y. Vardi, Maximum likelihood reconstruction for emission tomography, IEEE Trans. Med. Imaging 1 (2) (1982) 113–122.

[9] W. Guo, H. Chen, Improving SIRT algorithm for computerized tomographic image reconstruction, in: Z. Qian, L. Cao, W. Su, T. Wang, H. Yang (Eds.), Recent Advances in Computer Science and Information Engineering, vol. 128 of Lecture Notes in Electrical Engineering, Springer, Berlin, Heidelberg, 2012, pp. 523–528, http://dx.doi.org/10.1007/978-3-642-25792-6_79.

[10] L. Liu, Model-based iterative reconstruction: a promising algorithm for today's computed tomography imaging, J. Med. Imaging Radiat. Sci. 45 (2) (2014) 131–136, http://dx.doi.org/10.1016/j.jmir.2014.02.002.

[11] C. Ghetti, O. Ortenzia, G. Serreli, {CT} iterative reconstruction in image space: a phantom study, Physica Medica 28 (2) (2012) 161–165, http://dx.doi.org/10.1016/j.ejmp.2011.03.003.

[12] P. Delsanto, A. Romano, M. Scalerandi, F. Moldoveanu, Application of genetic **Q7** algorithms to ultrasonic tomography, J. Acoust. Soc. Am. 104 (3) (1998).

[13] X. Li, T. Jiang, D. Evans, Medical image reconstruction using a multi-objective genetic local search algorithm, Int. J. Comput. Math. 74 (2000) 301–314.

[14] S. Qureshi, S.M. Mirza, M. Arif, A hybrid continuous genetic algorithm for parallelray transmission tomography image reconstruction, J. Biomed. Inf. (2006).

[15] M. Rantala, S. Vanska, S. Jarvenpaa, M. Kalke, M. Lassas, J. Moberg, S. Siltanen, Wavelet-based reconstruction for limited-angle X-ray tomography, IEEE Trans. Med. Imaging 25 (2) (2006).

[16] F.P. Vidal, D. Lazaro-Ponthus, S. Legoupil, J. Louchet, E. Lutton, J.-M. Rocchisani, Artificial evolution for 3D pet reconstruction, in: P. Collet, N. Monmarch, P. Legrand, M. Schoenauer, E. Lutton (Eds.), Artificial Evolution, vol. 5975 of Lecture Notes in Computer Science, Springer, 2009, pp. 37–48, URL http://dblp.uni-trier.de/db/conf/ae/ae2009.html#VidalLLLLR09.

[17] A.M.T. Gouicem, K. Benmahammed, R. Drai, M. Yahi, A. Taleb-Ahmed, Multi-objective GA optimization of fuzzy penalty for image reconstruction from projections in X-ray tomography, Digit. Signal Process. 22 (3) (2012) 486–496, http://dx.doi.org/10.1016/j.dsp.2011.10.013.

[18] A. Ouaddah, D. Boughaci, Local search method for image reconstruction with same concentration in tomography, in: SIRS, 2014, pp. 335–346, http://dx.doi.org/10.1007/978-3-319-04960-1_30.

[19] J. Xu, X. Song, Ant colony optimization for nonlinear inversion of Rayleigh waves, in: Proceedings of the 7th International Conference on Intelligent Computing: Bio-inspired Computing and Applications, ICIC'11, Berlin, Heidelberg, Springer-Verlag, 2011, pp. 370–377, http://dx.doi.org/10.1007/978-3-642-24553-4_49.

[20] D. di Serafino, F. Riccio, On the application of multiple-DEME parallel genetic algorithms in astrophysics, in: Proceedings of the 2010 18th Euromicro Conference on Parallel, Distributed and Network-based Processing, PDP'10, IEEE Computer Society, Washington, DC, USA, 2010, pp. 231–237, http://dx.doi.org/10.1109/PDP.2010.70.

[21] G.K. Matsopoulos, K.K. Delibasis, N.A. Mouravliansky, P.A. Asvestas, K.S. Nikita, V.E. Kouloulias, N.K. Uzunoglu, CT-MRI automatic surface-based registration schemes combining global and local optimization techniques, Technol. Health Care 11 (4) (2003) 219–232, URL http://dl.acm.org/citation.cfm?id=1317285.1317286.

[22] J.J. Merelo, A. Prieto, F. Morán, R. Marabini, J.M. Carazo, Automatic classification of biological particles from electron-microscopy images using conventional and genetic-algorithm optimized learning vector quantization, Neural Process. Lett. 8 (1) (1998) 55–65, http://dx.doi.org/10.1023/A:1009617113191.

[23] P. Donald, K. Kihm, Tomographic-image reconstruction using a hybrid genetic algorithm, Opt. Lett. 22 (1997) 847–849.

[24] M. Lyra, A. Ploussi, Filtering in SPECT image reconstruction, J. Biomed. Imaging 2011 (2011) 10.1–10.14, http://dx.doi.org/10.1155/2011/693795.

[25] J. Greffier, A. Fernandez, F. Macri, C. Freitag, L. Metge, J.-P. Beregi, Which dose for what image? Iterative reconstruction for {CT} scan, Diagn. Interv. Imaging 94 (11) (2013) 1117–1121, http://dx.doi.org/10.1016/j.diii.2013.03.008.

[26] A. Mohammad-Djafari, Image reconstruction of a compact object from a few number of projections, in: IASTED, Int. Conf. on Signal and Image Processing (SIP'96), 1996, pp. 325–329.

[27] A. Sakari, Reconstruction from projections, 7103100 Lketieteelliset kuvaus-menetelmt, 2003.

[28] M.N. Asl, A. Sadremomtaz, Analytical image reconstruction methods in emission tomography, J. Biomed. Sci. Eng. 6 (1) (2013), http://dx.doi.org/10.4236/jbise.2013.61013.

[29] P. Bruyant, Analytic and iterative reconstruction algorithms in SPECT, J. Nucl. Med. 43 (2002) 1343–1358.

[30] J. Radon, On the determination of functions from their integrals along certain manifolds, Math. Phys. Klass. 69 (1917) 262–277 (in German).

[31] A. Kak, Image reconstruction from projections Image Processing Techniques, Computational Techniques, vol. 2, Academic Press, 1984, pp. 111–169.

[32] Y. Ye, H. Yu, G. Wang, Exact interior reconstruction with cone-beam CT, **Q8** J. Biomed. Imaging 2007 (3) (2007) 1.1–1.5, http://dx.doi.org/10.1155/2007/10693.

[33] H.M. Hudson, R.S. Larkin, Accelerated image reconstruction using ordered subsets of projection data, IEEE Trans. Med. Imaging 13 (4) (1994) 601–609.

[34] Z.W. Geem, J.-H. Kim, G.V. Loganathan, A new heuristic optimization algorithm: harmony search, Simulation 76 (2) (2001) 60–68, URL http://dblp.uni-trier.de/db/journals/simulation/simulation76.html#GeemKL01.

[35] S. Bathaee, M. Fesanghary, A. Vasebi, M. Hassani Keleshtery, A new stochastic algorithm for various types of economic dispatch problems, in: Harmony Search. The 8th International Power Engineering Conference – IPEC2007, 2007.

[36] M. Mahdavi, M. Fesanghary, E. Damangir, An improved harmony search algorithm for solving optimization problems, Appl. Math. Comput. 188 (2) (2007) 1567–1579, http://dx.doi.org/10.1016/j.amc.2006.11.033.

[37] Z.W. Geem, Harmony search algorithm for solving sudoku, in: Proceedings of the 11th International Conference, KES 2007 and XVII Italian Workshop on Neural Networks Conference on Knowledge-based Intelligent Information and Engineering Systems: Part I, KES'07/WIRN'07, Springer-Verlag, Berlin, Heidelberg, 2007, pp. 371–378, URL http://dl.acm.org/citation.cfm?id=1771110.1771162.

[38] Z.W. Geem, Harmony search algorithms for structural design optimization, in: Stud. Comput. Intell., Springer, Berlin, Heidelberg, 2009, p. 239, http://dx.doi.org/10.1007/978-3-642-03450-3.

[39] O.M. Alia, R. Mandava, The variants of the harmony search algorithm: an overview, Artif. Intell. Rev. 36 (1) (2011) 49–68, http://dx.doi.org/10.1007/s10462-010-9201-y.

[40] L. Wang, R. Yang, Y. Xu, Q. Niu, P.M. Pardalos, M. Fei, An improved adaptive binary harmony search algorithm, Inf. Sci. 232 (2013) 58–87, http://dx.doi.org/10.1016/j.ins.2012.12.043.

[41] G.T. Herman, A. Lent, Iterative reconstruction algorithms, Comput. Biol. Med. 6 (4) (1976) 273–294, http://dx.doi.org/10.1016/0010-4825(76)90066-4.

[42] A. Vadivel, A. Majumdar, S. Sural, Performance comparison of distance metrics in content-based image retrieval applications, in: International Conference on Information Technology (CIT), 2003, pp. 159–164.

[43] Z. Wang, A.C. Bovik, Mean squared error: love it or leave it? a new look at signal fidelity measures, IEEE Signal Process. Mag. 26 (1) (2009) 98–117, http://dx.doi.org/10.1109/MSP.2008.930649.

[44] Q. Huynh-Thu, M. Ghanbari, Scope of validity of PSNR in image/video quality assessment, Electron. Lett. 44 (13) (2008) 800–801, http://dx.doi.org/10.1049/el:20080522.